RESEARCH

Targeting osteoclast-derived DPP4 alleviates inflammation-mediated ectopic bone formation in ankylosing spondylitis

Seung Hoon Lee[1†], Kyu Hoon Lee[2†], Dongju Kim[1], Chanhyeok Jeon[1], Min Whangbo[1], Hye-Ryeong Jo[1], Jeehee Youn[3], Chang-Hun Lee[4], Sung Hoon Choi[4], Ye-Soo Park[5], Bora Nam[6], Sungsin Jo[7*] and Tae-Hwan Kim[1,6*]

Abstract

Background Ankylosing spondylitis (AS) is a chronic inflammatory disease characterized by ectopic bone formation. The anti-inflammatory function of dipeptidyl peptidase-4 (DPP4) inhibitor has been reported in bone metabolism, but its utility in AS has not previously been investigated.

Methods We assessed DPP4 level in serum, synovial fluid, and facet joint tissue of AS patients. Additionally, we investigated the effect of a DPP4 inhibitor in an experimental AS model using curdlan-injected SKG mice. Following curdlan injection, SKG mice were orally administered a DPP4 inhibitor three times per week for 5 weeks and observed clinical arthritis scores, and analyzed by micro-CT. Furthermore, osteoclast precursor cells (OPCs) from curdlan-injected SKG mice were treated with DPP4 inhibitor and evaluated the inhibitory effects of this treatment in vitro.

Results Soluble DPP4 level was elevated in the serum and synovial fluid of patients with AS compared to those in the control group. Expression of DPP4 increased gradually during human osteoclastogenesis and was high in mature osteoclasts. Oral administration of a DPP4 inhibitor resulted in a decrease in thickness of the hind paw, clinical arthritis scores, and enthesitis at the ankle in curdlan-injected SKG mice compared to the vehicle group. Micro-CT data revealed a significant reduction in inflammation-induced low bone density in the DPP4 inhibitor group. Moreover, treatment with a DPP4 inhibitor significantly reduced osteoclast differentiation of OPC in addition to decreasing expression of osteoclast differentiation markers.

Conclusion Our findings suggest that inhibiting DPP4 may have a therapeutic effect on inflammation-mediated ectopic bone formation in AS patients.

Keywords Dipeptidyl peptidase-4 (DPP4) inhibitor, Osteoclasts, Curdlan-injected SKG mice, Inflammation-mediated ectopic bone formation

---

†Seung Hoon Lee and Kyu Hoon Lee contributed equally to this work.

*Correspondence:
Sungsin Jo
joejo0517@sch.ac.kr
Tae-Hwan Kim
thkim@hanyang.ac.kr
Full list of author information is available at the end of the article

Lee *et al. Arthritis Research & Therapy*   (2025) 27:40

Page 2 of 13

Background

Ankylosing spondylitis (AS) is a chronic inflammatory disease that affects the joints and enthesis in the axial skeleton [1, 2]. Clinically, TNF or IL-17 inhibitors can reduce inflammation and slow the progression of ankylosis [3–7]. Pathophysiologically, animal models for inflammatory arthritis revealed that local inflammation triggers bone erosion with increased osteoclasts, leading to bone formation emerged by osteoblasts. This phase eventually induces ectopic/new bone formation, resulting in the formation of bony bridges and spinal ankylosis [8–10]. Indeed, chronic inflammation causing imbalance between osteoclast and osteoblast activity or excessive osteoproliferation/bone-forming activity is considered the main mechanism underlying ectopic/new bone formation of AS [11]. Recent studies have shown that active osteoclasts are present in ectopic bone in AS and could contribute to the progression of ectopic bone formation [12, 13]. Therefore, factors derived from active osteoclasts could potentially trigger excessive osteoblast activity, leading to the onset and progression of AS.

Osteoclasts are responsible for bone resorption and play a crucial role in bone remodeling and homeostasis [14]. Osteoclast precursor cells (OCPs) are derived from CD14-positive monocytes of peripheral mononuclear cells (PBMCs) in vitro. OCPs differentiate into osteoclasts upon stimulation by two key ligands: macrophage colony-stimulating factor (M-CSF) and receptor activator of nuclear factor kappa-B ligand (RANKL) [15, 16]. Binding of RANKL to the receptor activator of nuclear factor kappa-B (RANK/TNFRSF11a) induces nuclear factor-activated T cells c1 (NFATc1), which plays a crucial role in osteoclastogenesis and the maturation of osteoclasts. In particular, osteoclast-derived coupling factors not only control bone remodeling but are also associated with bone-related diseases [17–20].

Dipeptidyl peptidase-4 (DPP4) is a widely expressed multifunctional serine peptidase that exists as a membrane-anchored cell surface protein or in soluble form in the plasma [21]. Soluble DPP4 elevates pro-inflammatory cytokines (IL-6 and IL-8) and induces inflammation through the activation of MARK-and NF-κB signaling pathway [22, 23]. Indeed, it is an adipokine that plays a crucial role in the development of obesity and insulin resistance [24], both of which have been suggested to be involved in the pathogenesis of osteoporosis [25]. Interestingly, DPP4 inhibitors have been shown to reduce the risk of bone fracture based on meta-analyses of randomized clinical trials [26–28]. DPP4 expression is highly expressed in human osteoclasts [29], and DPP4 inhibitors have been shown to reduce osteoclast differentiation and bone resorption in vivo [30, 31]. There is not only limited literature on association of DPP4 inhibitors with bone metabolism [32], but not yet fully explored in the DPP4 in AS.

In this study, we observed significant elevation of DPP4 level in the serum and synovial fluid of patients with AS compared to the control group. We also demonstrated that expression of DPP4 in mature osteoclasts and DPP4 inhibitor reduced arthritis, enthesitis, and ectopic bone formation in the ankles of curdlan-injected SKG mice in vivo as well as of osteoclast differentiation in vitro.

Methods

Sample collection and DPP4 measurement

This study was approved by the ethics committee of Hanyang University Seoul Hospital, and written informed consent was obtained from all study participants (2014-05-001, 2014-05-002). All patients with AS enrolled in this study fulfilled the evaluation of 1984 modified New York criteria for AS [33]. All serum were male, and serum were collected from twenty-six healthy control (HC) donors and thirty patients with AS.

Synovial fluid of osteoarthritis (OA) met the criteria for knee OA [34]. Synovial fluids were collected from knee joints in seven patients with OA (2 males and 5 females) and twenty-four patients with AS (15 males and 9 females).

Facet bone tissues were obtained from five patients without inflammatory disease (all males) and five patients with AS (all males).

DPP4 levels in serum and synovial fluid were determined using a commercial ELISA kit (RK02755; ABclonal) according to the manufacturer's protocol.

Immunohistochemistry

Immunohistochemistry was performed as described previously in detail [35, 36]. Briefly, 5-μm paraffin-embedded sections of facet joints were deparaffinized and permeabilized. Endogenous peroxidase was eliminated, and antigen retrieval was performed using proteinase K solution (ab64220; abcam). Slides were incubated with a primary antibody against DPP4 (A1455; ABclonal, antibody dilution; 1:100, temperature and incubation time; 4℃ for overnight), followed by incubation of secondary antibody, amplification, and visualization using an EnVision Detection System kit (K5007; DaKo). Stained slides were mounted and visualized under microscope (Ti-U; Nikon, Tokyo, Japan). To quantify the expression of DPP4, the number of positively stained cells was determined among the total number of cells in three random fields. High-power fields were observed at 200x magnification.

Differentially expressed genes (DEG) analysis

GSE225974, independent public dataset, was reanalyzed at the Research Support Center for Bio-Bigdata Analysis

Lee *et al. Arthritis Research & Therapy*   (2025) 27:40

Page 3 of 13

Human CD14 isolation and osteoclasts differentiation

Human and murine osteoclast precursor cells (OCP) isolation and osteoclast differentiation were performed as described previously [37, 38]. Human peripheral blood monocytes (PBMC) were isolated from the blood of healthy donors using Ficoll gradient centrifugation (17–1440-03; GE Healthcare). Monocytes were purified from PBMCs using CD14-positive magnetic beads (130-050-201; Miltenyi Biotec) according to the manufacturer's instructions. Briefly, human peripheral blood mononuclear cells (PBMC)/CD14+cells were cultured in 20 ng/mL human M-CSF (300−25; Peprotech) in α-MEM medium (Gibco) including 10% FBS (Gibco) and 1% penicillin/streptomycin (Gibco) for 2 days to generate osteoclast precursor cells (OCPs). Then, OCPs were incubated with 20 ng/mL M-CSF and 40 ng/mL RANKL (310-01; Peprotech) for an additional 6 days. Culture medium was replenished every 3 days. Murine bone marrow cells were obtained from femurs and tibias of curdlan-injected SKG mice and were treated with ACK lysis buffer (A10492-01; Gibco) to remove RBCs and cultured on dishes with 10 ng/mL murine M-CSF (315-02; Peprotech) for 1 day. Then, suspension cells were collected and further cultured with 20 ng/mL murine M-CSF for 1 day, followed by treatment with 50 ng/mL M-CSF and 100 ng/mL RANKL (315−11; Peprotech) for 4 days. The culture medium was replaced every 3 days.

At the end of the culture period, mature osteoclasts were fixed in 10% formalin and stained for acid phosphatase 5, tartrate resistant (TRAP) using a commercial kit (PMC-AK04-COS; CosmoBio) according to the manufacturer's protocol. TRAP+osteoclasts (more than three nuclei) were counted. To detect F-actin ring formation, cells were fixed and permeabilized with 0.1% Triton X-100 and then incubated with FITC-conjugated phalloidin (P5282; Sigma- Aldrich) for 60 min at 37 °C. Images of stained cells were collected under a microscope equipped with a camera (Ti-U; Nikon, Tokyo, Japan).

RNA extraction and mRNA analysis

RT-PCR and qPCR were performed as previously described [36]. Primers used for RT-qPCR reactions were as follows: hTRAP-qF, TGGCTTTGCCTATGT GGA; hTRAP-qR, CCTGGTCTTAAAGAGGGACTT; mTRAP-qF, ACGGCTACTTGCGGTTTC; mTRAP-qR, TCCTTGGGAGGCTGGTC; hCTK-qF, CTCTTCCAT TTCTTCCACGAT; hCTK-qR, ACACCAACTCCCTTC CAAAG; mCTK-qF, AAGATATTGGTGGCTTTGG; mCTK-qR, ATCGCTGCGTCCCTCT; hITGB3-qF, GGA AGAACGCGCCAGAGCAAAATG; hITGB3-qR, CCC CAAATCCCTCCCCACAAATAC; mITGB3-qF, GAA ACAGAGCGTGTCCCGTA; mITGB3-qR, GGTCTT GGCATCCGTGGTAA; hDC-STAMP-qF, AAAGCT TGCCAGGGTTTGAG; hDC-STAMP-qR, GGTTTT GGGATACAGTTGGGTTC; mDC-STAMP-qF, TCC TCCATGAACAAACAGTT; mDC-STAMP-qR, AGA CGTGGTTTAGGAATGCA; hNFATc1-qF, GCATCA CAGGGAAGACCGTGTC; hNFATc1-qR, GAAGTT CAATGTCGGAGTTTCTGAG; mNFATc1-qF, CCC GTCACATTCTGGTCCAT; mNFATc1-qR, CAAGTA ACCGTGTAGCTCCACAA; hDPP4-qF, GACACCGTG GAAGGTTCTTCT; hDPP4-qR, CTGTAGCATCAT CTGTGCCTT; hGAPDH-qF, ATCAAGAAGGTGGTG AAGCA; hGAPDH-qR, GTCGCTGTTGAAGTCAGA GGA; mβ-Actin-qF, CCTGAACCCTAAGGCCAACC; mβ-Actin-qR, ATGGCGTGAGGGAGAGCATA.

Protein extraction and immunoblotting analysis

Immunoblotting was performed as described previously with minor modifications [13, 39]. Briefly, cell pellets were lysed in 1X RIPA buffer including protease and phosphatase inhibitor cocktails and incubated on ice for 1 h followed by a centrifugation at 12,000 g for 30 min at 4 °C. About thirty lysates were separated by SDS-PAGE and electrophoretically transferred to nitrocellulose membranes (10600002; GE Healthcare) in a prechilled 1X transbuffer (temperature and transfer time; at 4℃ for two hour). Membranes were blocked with 5% non-fat milk in Tris-buffered saline (TBS) with 0.1% Tween-20 for an hour and incubated with specific primary antibodies (temperature and transfer time; 4℃ for overnight), followed by incubation with horseradish peroxidase-conjugated secondary antibodies (temperature and transfer time; room-temperature for an hour). Immunoblots were visualized with *Pierce ECL (32106; ThermoFisher), followed by* UVITECH imaging System (Cambridge UK).

Primary antibodies against NFATc1 (556602; BD Biosciences), DPP4 (A1455; ABclonal), phosY527 SRC (2105; Cell Signaling), phos-Y416 SRC (2101; Cell Signaling), total SRC (2108; Cell Signaling), phos-p38 (9215; Cell Signaling), total-p38 (sc-535; Santa Cruz), phos-ERK (9102; Cell Signaling), phos-JNK (9255; Cell Signaling), ALP (sc-365765; Santa Cruz), COL1A (sc-59772; Santa Cruz), OPN (sc-21742; Santa Cruz), OCN (ab93876; abcam), RUNX2 (12556; Cell Signaling), GAPDH (5174; Cell Signaling), and β-actin (A2228; Sigma) were used. Horseradish peroxidase (HRP)-conjugated secondary antibodies (111-035-003 and 115-035-003; from Jackson Immune Research) were used. Primary antibodies were diluted 100-fold in 1X TBS-T and secondary antibodies were diluted 500-fold in 1X TBS-T with 5% non-fact milk for immunoblotting experiments.

Lee *et al. Arthritis Research & Therapy* (2025) 27:40

Page 4 of 13

Immunofluorescence

Cells were seeded onto glass coverslips in 24-well plates at 5×10^4 cells per well. The next day, cells were rinsed with ice-cold PBS and fixed with 4% paraformaldehyde in PBS. Following cell fixation, cells were blocked with blocking solution (0.3% Triton X-100, 1% bovine serum albumin, and 10% normal goat serum in PBS) for 1 h at room temperature. Cells were incubated with appropriate primary antibodies (1:100) in blocking solution for overnight at 4ºC and then with Cy3-conjugated anti-rabbit antibody (111–165-144; Jackson ImmunoResearch Laboratories) or Alexa Fluor 594-conjugated anti-mouse antibody (A-11005; Thermo Fisher Scientific) for an hour at room-temperature. The stained slide was mounted with VECTASHIELD Mounting Medium with DAPI (H-1200; Vector Laboratories). Immunofluorescence images were acquired by confocal microscopy (Leica Microsystems, Germany).

Curdlan-injected SKG mice

All experimental procedures were performed in accordance with the Guide for the Care and Use of Laboratory Animals and were approved by the Animals Ethics Screening Committee of Hanyang University (2022–0027 A). ZAP-70 mutant SKG mice derived from BALB/c strain were originally obtained from Dr. Sakaguchi (Osaka University, Japan) [40]. Eight-week-old male SKG mice (total $n = 20$) were intraperitoneally injected with 3 mg of curdlan [41]. One week later, SKG mice were randomly divided into two groups ($n = 8$ mice for each group). One group received PBS injections, while the other received oral administration with 30 μg of DPP4 inhibitor (known as Linagliptin, S3031; Selleckchem) three times weekly for 5 weeks. All mice were monitored for up to 5 weeks and scored by the same observer, who was blinded, as follows: 0 = no swelling or redness, 0.1 = swelling or redness of digits, 0.5 = mild swelling and/or redness of wrists or ankle joints, and 1 = severe swelling of the larger joints. Scores of the affected joints were summed, with a maximum possible score of 6 [42]. Histopathological features of mouse ankles were scored on a scale of 1–4, where 1 = few infiltrating immune cells, 2 = 1–2 small patches of inflammation, 3 = inflammation throughout the ankle joint, and 4 = inflammation in soft tissue/entheses/fasciitis [41]. To quantitatively evaluate the severity of enthesitis, mouse paws were scored using a previously described scoring system where 1 = mild inflammation at the tendon insertion site, 2 = mild-to moderate inflammatory infiltrate at the insertion site and along the tendon, 3 = severe inflammation with bone involvement, and 4 = severe inflammation with obliteration of the tendon-bone interface [43]. Mice were sacrificed, and their femurs and tibia were collected to isolate bone marrow cells for osteoclast differentiation.

Histological and micro-CT analysis

Ankles of sacrificed mice were fixed with 10% formalin for 1 week and decalcified with 20% EDTA for at least 1 month at 4 °C. Paraffin-embedded tissue blocks were sectioned at 5-μm thickness. Sections were used for histological analysis and osteoclasts for TRAP examination. Staining procedures were conducted in accordance with standard protocols or the manufacturer's instructions. The slides were stained with hematoxylin and eosin (H&E, 1.05174.0500; Merck) for histological observation, Safranin O solution (SO, ab150681; Abcam) for cartilage analysis, and TRAP for osteoclast analysis. All slides were mounted with permanent mounting medium (H-5000; Vector Lab).

Micro-computed tomography (Micro-CT) analyses were conducted, and data were analyzed by the 2nd Analysis Lab (Seoul, Korea). Mouse ankles were fixed in 10% formalin for 1 week and analyzed by high-resolution Micro-CT (Skyscan1272; Bruker Micro-CT, Kontich, Belgium). Scanner settings were as follows: voltage of 60 kV, aluminum filter of 0.25 mm, and a resolution of 9 μm per pixel. The Micro-CT images were used for three-dimensional (3D) histomorphometric analyses. Images were reconstructed with NRecon v1.7.3.1 software (Bruker Micro-CT)+InstaRecon software (InstaRecon), analyzed by CTAn v1.20.3.0 software (Bruker Micro-CT), and visualized using the 3D model visualization software CTVol v2.3.2.0 (Bruker Micro-CT).

Human osteoprogenitor cell isolation and osteoblast differentiation

The method for osteoblast differentiation of human primary osteoprogenitor cells was previously described in detail [42]. The primary osteoprogenitor cells were isolated from human cancellous bone chips and cultured in DMEM (SH30243.01; HyClone) growth medium (GM) containing 10% FBS (16,000–044; Gibco) and 1% penicillin/streptomycin (15,140–122; Gibco). The isolated cells were induced to osteoblast differentiation with osteogenic conditional medium (OM) based on GM containing 50 μM ascorbic acid (A4544; Sigma), 10 mM β-glycerolphosphate (SC-220452 A; Santa Cruz), and 100 nM dexamethasone (D2915; Sigma). The OM was replaced every 3 days. During osteoblast differentiation, at 7 days, matrix maturation was evaluated by alkaline phosphatase (ALP) and type 1 collagen (COL) staining. At 14 and 21 days, matrix mineralization was evaluated using alizarin red (ARS), von kossa (VON), and hydroxyapatite (HA) staining.

Statistics analysis

Graph-Pad Prism 7 was used to produce graphs and to conduct statistical analyses. The Mann-Whitney test or Student's t-test was performed to assess the statistical significance of differences between groups. Prior to this, normality tests (Shapiro-Wilk test) were conducted to determine whether the data followed a normal distribution. When more than two groups were compared, either one-way ANOVA was used. Values are presented as mean ± standard error of the mean (SEM). All experiments were conducted at least three times. Asterisks represent the level of statistical significance (* $p < 0.05$, ** $p < 0.01$, *** $p < 0.001$).

Results

DPP4 expression is elevated in the serum, synovial fluid, and facet joint tissue samples of AS patients

We first examined the DPP4 level in collected human serum and synovial fluid of AS patients and compared it to that in control patients. All serum were male, and serum were collected from twenty-six healthy control (HC) donors (32.1 ± 5.2 years) and thirty patients with AS (mean age 37.3 ± 2.6 years). In patients with AS, levels of erythrocyte sedimentation rate (ESR) and C-reactive protein (CRP) were 40.33 ± 36.1 mm/h and 3.15 ± 2.6 mg/dl, respectively. Synovial fluids were collected from knee joints in seven patients with OA (61.4 ± 6.7 years) and twenty-four patients with AS (47.7 ± 16.5 years). In patients with AS, the levels of ESR and CRP were 41.1 ± 35.5 mm/h and 4.7 ± 5.8 mg/dl, respectively. ESR and CRP levels in OA patients were measured close to the normal value of O. Soluble DPP4 was significantly elevated in serum (Fig. 1A) and synovial fluid (Fig. 1B) samples of AS patients. Given this finding, we next examined expression of DPP4 in the facet joints within L-spine tissues of AS patients. Facet bone tissues were obtained from five patients without inflammatory disease (mean age 49.6 ± 5.5 years) and five patients with AS (mean age 50.6 ± 5.4 years). In patients with AS, the levels of ESR and CRP were 15.4 ± 14.5 mm/h and 4.0 ± 1.9 mg/dl, respectively. Immunohistochemistry analysis and immunofluorescence analysis revealed that DPP4 expression was higher in inflammatory immune cells of the bone marrow region within facet joints of AS patients than control patients (Fig. 1C-F). These results indicate that DPP4 expression is elevated in AS patients.

DPP4 is highly expressed in human mature osteoclasts

Recently, Weivoda and colleagues reported that DPP4 is highly expressed in bone marrow-derived osteoclasts [30] and GSE225974, independent public dataset, was reanalyzed to reveal an increase of DPP4 in human osteoclasts (Fig. 2A and Suppl. Figure 1 A). To test whether DPP4 is expressed by osteoclasts, we differentiated osteoclasts from human CD14-positive monocytes of human blood as shown in Fig. 2B. Human mature osteoclasts at 9 days were well-formed, as determined by TRAP and F-actin assays (Fig. 2C). NFATc1 protein level was upregulated in mature osteoclasts at 9 days, and DPP4 protein level increased gradually during osteoclastogenesis (Fig. 2D). RT-qPCR data indicated that DPP4 mRNA expression was gradually upregulated during osteoclastogenesis in addition to levels of osteoclast differentiation markers such as tartrate-resistant acid phosphatase (TRAP), cathepsin K (CTK), integrin beta chain beta 3 (ITGB3), and dendritic cell-specific transmembrane protein (DC-STAMP) (Fig. 2E). Consistent with the previous observation [29, 30], DPP4 was highly expressed in human osteoclasts compared to PBMC (Suppl. Figure 1B). Using immunofluorescence, we also confirmed DPP4 expression in human mature osteoclasts (Fig. 2F). These findings indicate that DPP4 is highly expressed by mature human osteoclasts.

Treatment with DPP4 inhibitor reduces arthritis and enthesitis, and inflammation in the peripheral joints of curdlan-injected SKG mice in vivo

Since we found high level of DPP4 in AS patients, we experimentally designed the effects of oral administration with DPP4 inhibitor in a curdlan-injected SKG mice model (Fig. 3A). As comparison of DPP4 inhibitor group with vehicle group in curdlan-injected SKG mice, oral administration with DPP4 inhibitor dramatically alleviated clinical symptoms such as arthritis scores, hind paw thickness after 3 weeks in curdlan-injected SKG mice (Fig. 3B). Dactylitis in foots and ectopic bone formation in ankle (indicated as black arrows) were obviously decreased in DPP4 inhibitor group of curdlan-injected SKG mice (Fig. 3C). Moreover, DPP4 inhibitor group showed reduction of popliteal lymph node size in curdlan-injected SKG mice (Suppl. Figure 2). Histological analysis exhibited decreased inflammation in the bone marrow and enthesitis within ankle of the DPP4 inhibitor group compared to the curdlan-injected SKG mice group (Fig. 3D and E). Proinflammatory cytokines such as TNFα, IL-1β, and IL-6 were statistically reduced in ankle region of DPP4 inhibitor group compared to vehicle group (Suppl. Figure 3). Micro-CT analysis revealed that mice treated with the DPP4 inhibitor had statistically reduced inflammation-mediated ectopic bone formation and low bone density in their foot (Fig. 3F; indicated as red arrows and 3G). Taken together, these data confirm that treatment with DPP4 inhibitor significantly decreased arthritis, enthesitis, and ectopic bone formation in the peripheral joints of curdlan-injected SKG mice.
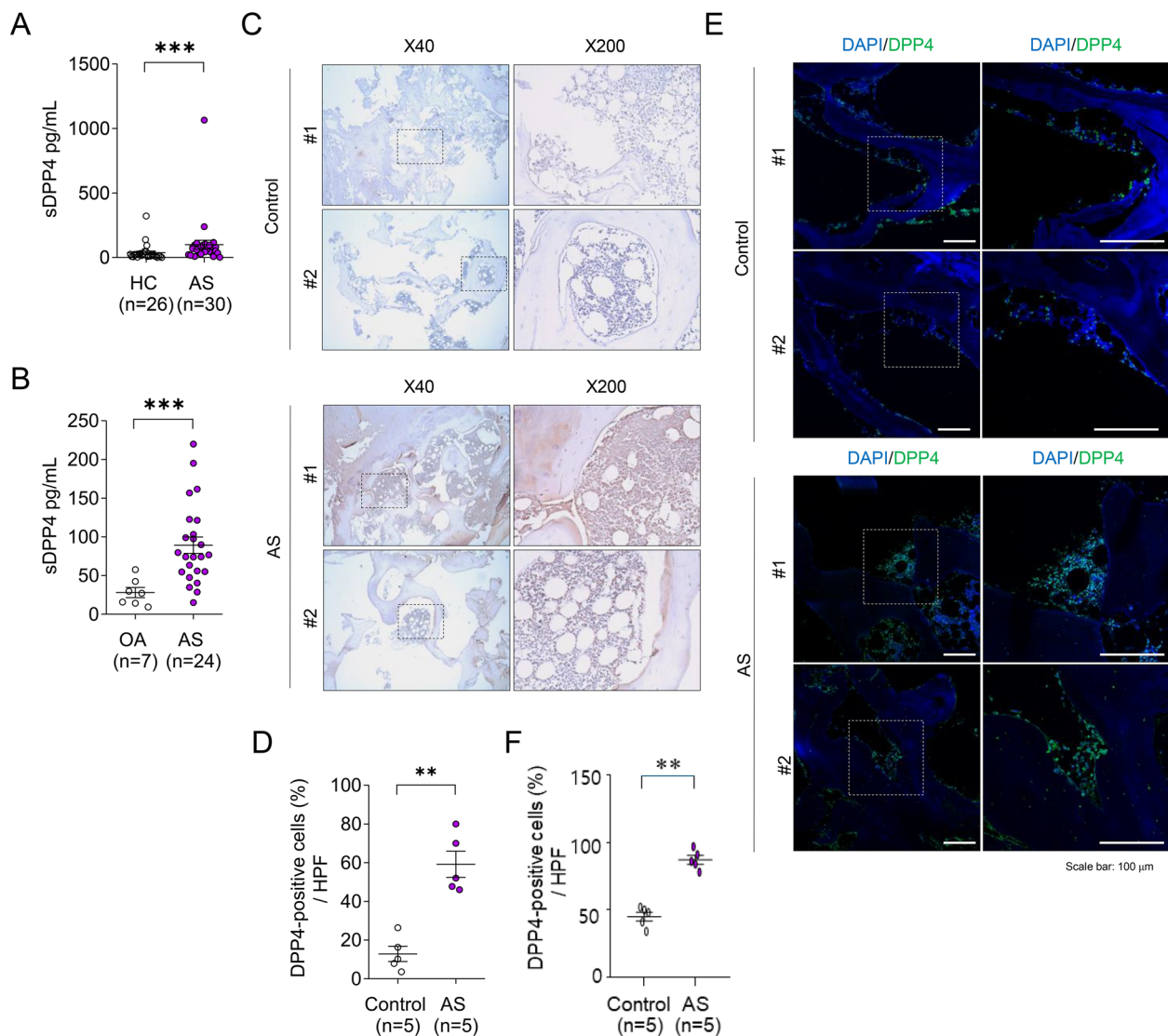
Lee *et al. Arthritis Research & Therapy*   (2025) 27:40

Page 6 of 13

Fig. 1 Expression of DPP4 is significantly elevated in AS. We measured soluble DPP4 level in serum and synovial fluid. Soluble DPP4 level was assessed by ELISA in (**A**) the serum of healthy control participants (HC; $n = 26$) and patients with AS ($n = 30$) and in (**B**) synovial fluid samples from patients with osteoarthritis (OA; $n = 7$) and AS ($n = 24$). Immunohistochemical staining (**C**) and immunofluorescence staining (**E**) for DPP4 was performed on facet joint tissues from control ($n = 5$) and AS ($n = 5$) patients. Representative images are shown. **D** and **F** DPP4-positive cells were counted and quantified by two independent researchers. Statistical significance is shown by **$p < 0.01$, ***$p < 0.001$ based on the Mann–Whitney U test

Treatment with DPP4 inhibitor diminishes ectopic bone formation in ankle of curdlan-injected SKG mice in vivo and attenuates osteoclast differentiation in vitro

Consistently, there was no difference of normal bone density in ankle between vehicle and DPP4 inhibitor treated groups, but ectopic bone formation and low bone density in ankle were significantly reduced by treatment with DPP4 inhibitor (Fig. 4A; indicated as red arrow and 4B). Interestingly, histologic analysis of the ankles of curdlan-injected SKG mice showed elevation in the percentages of TRAP-positive cells around hypertrophic chondrocytes

(Fig. 4C; indicated as black arrows), whereas DPP4 inhibitor group showed a significant reduction in ectopic bone formation as well as TRAP-positive cells ratio in the ankle (Fig. 4D). Furthermore, expressing DPP4 in TRAP-positive osteoclasts were enriched of AS facet joints that had undergone bone remodeling (Suppl. Figure 5; indicated as black arrows in H&E image and white arrows in immunofluorescence). To explore whether DPP4 inhibitor treatment affected osteoclastogenesis, we isolated bone marrow cells of curdlan-injected SKG mice and treated these murine osteoclast precursor cells
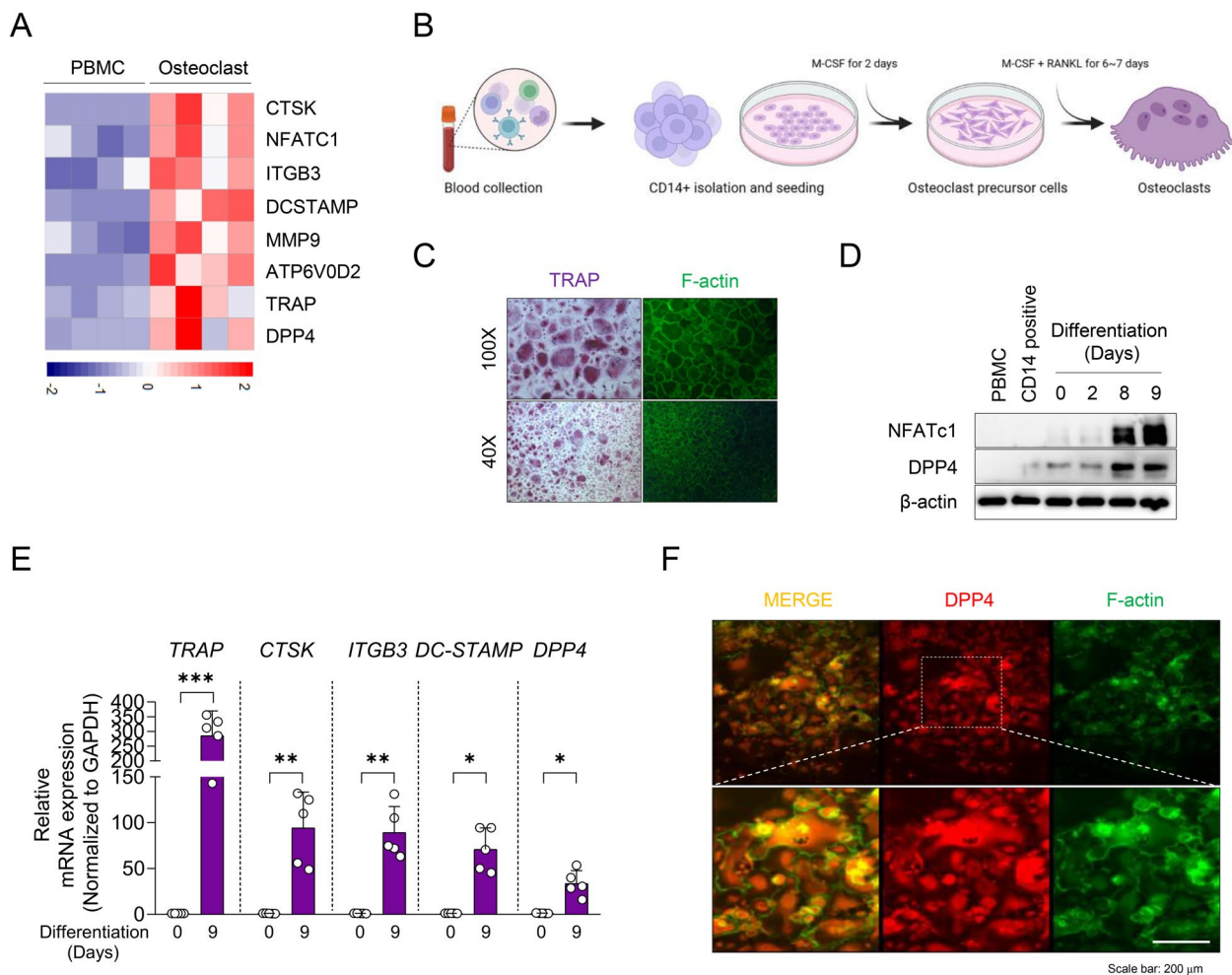
Fig. 2 DPP4 expression is highly expressed in human mature osteoclasts. **A** Osteoclast-related genes were analyzed by RNA-sequencing (GSE225974), and a heatmap was generated to compare the expression of osteoclast-related genes and DPP4 between peripheral blood mononuclear cell (PBMC) (*n* = 4) and osteoclast (*n* = 4) groups. **B** Schematic graphic illustrating the isolation of CD14 + cells from human PBMCs and their differentiation into mature osteoclasts in the presence of M-CSF (20 ng/mL) for 2 days followed by co-stimulation with M-CSF (20 ng/mL) and RANKL (40 ng/mL) for an additional 6–7 days. Figure was created with BioRender.com. Mature osteoclasts were subjected to (**C**) staining with TRAP and F-actin ring on day 8, (**D**) immunoblotting for NFATc1, DPP4, and β-actin as loading control, (**E**) RT-qPCR for osteoclast markers including TRAP, CTSK, ITGB3, DC-STAMP, and DPP4 (normalized to expression of GAPDH). **F** DPP4 localization in mature osteoclasts was observed by immunofluorescence, with DPP4 shown in red and F-actin in green. Statistical significance is shown by *$p < 0.05$, ***$p < 0.001$ based on the Mann–Whitney U test

(OPCs) with a DPP4 inhibitor. Treatment with the DPP4 inhibitor decreased the number of TRAP-positive osteoclasts (Fig. 4E and F) as well as osteoclast differentiation markers such as ITGB3, DC-STAMP, NFATc1, CTK, and TRAP (Fig. 4H). DPP4 inhibitor treatment also inhibited expression of NFATc1 in murine osteoclasts accompanied by decrease in phos-p38 and phos-Y527 SRC protein expression as revealed by immunoblotting (Fig. 4G). Collectively, these data demonstrate that treatment with DPP4 inhibitor diminishes ectopic bone formation in ankle of curdlan-injected SKG mice in vivo and attenuates osteoclast differentiation in vitro.

Discussion

This study highlights the potential therapeutic effect of DPP4 inhibitor treatment on ectopic bone formation in AS in vivo and in vitro. We found that increase in level and expression of DPP4 in serum, synovial fluid, and facet joint tissue samples of AS patients compared to control. We also showed high expression of DPP4 in mature osteoclasts. In vivo experiments using curdlan-injected SKG mice showed that targeting DPP4 significantly alleviated arthritis, dactylitis, inflammation, and ectopic bone formation in peripheral joints. In vitro experiments revealed that the DPP4 inhibitor reduced
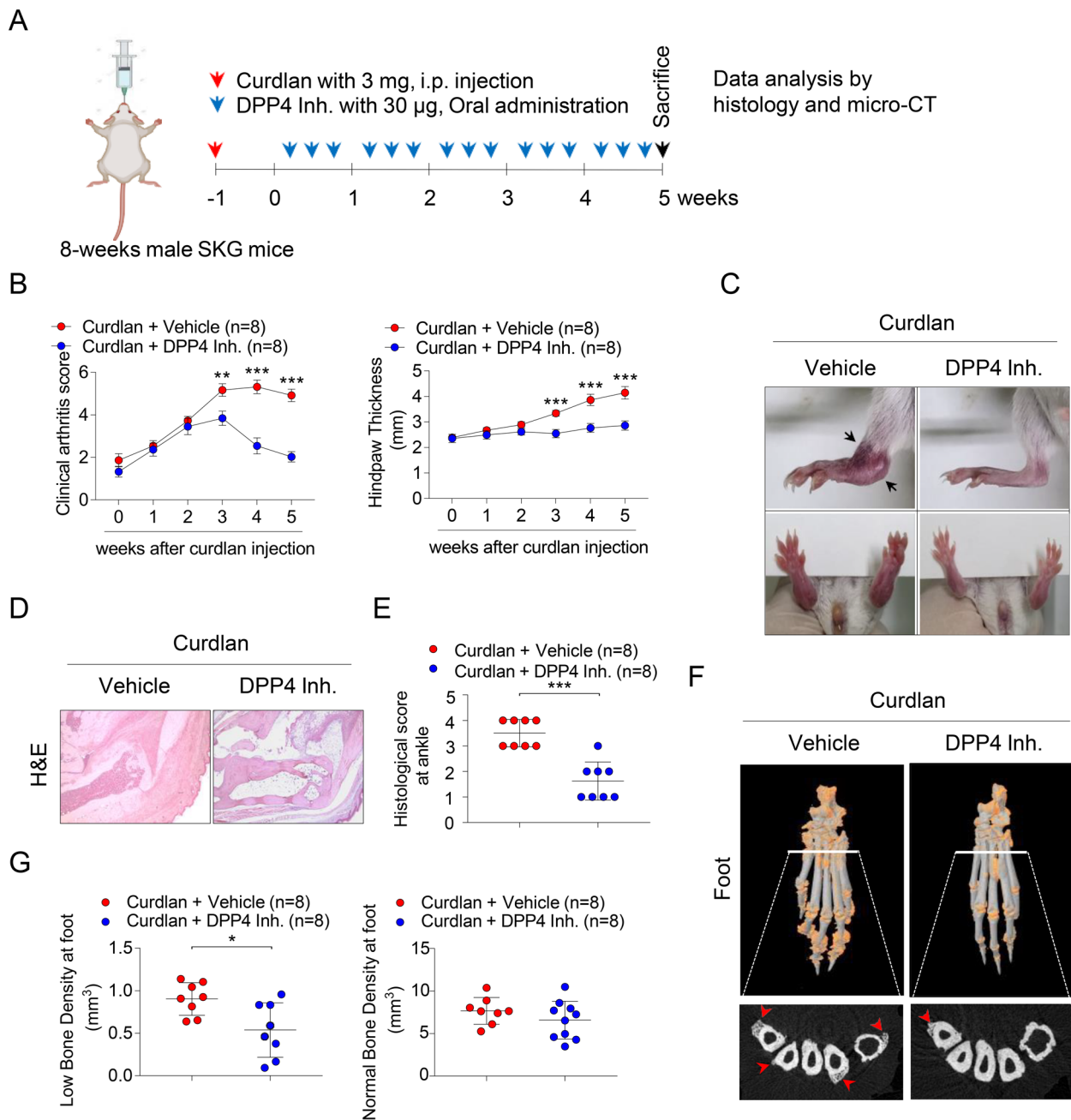
Fig. 3 Oral administration of DPP4 inhibitor attenuates arthritis, enthesitis, and inflammation in the peripheral joints of curdlan-injected SKG mice. Eight-week-old male SKG mice (total $n = 20$) were intraperitoneally injected with 3 mg of curdlan. After 1 week, SKG mice were randomly divided into two groups ($n = 8$ mice per group) and received oral administration of either PBS or of DPP4 inhibitor three times per week for 5 weeks. At the end of the 5 weeks, mice were sacrificed for further experiments. Experimental design is shown in (**A**). **B** Clinical arthritis scores and hind paw thickness were quantified. **C** Representative gross images of ankles and hind paws are displayed; blocked arrows indicate ectopic bone. **D** Histological images of ankle tissues stained with H&E that received histological scores ($n = 8$ mice per group). **E** Histological score at ankle were quantified as shown in (**D**). **F** Representative Micro-CT images of hind paws are shown, with orange and red arrows indicating low density bone and ectopic bone formation at peripheral joints, respectively. **G** Micro-CT image data were quantified as shown in (**F**). Statistical significance is shown by *$p < 0.05$, **$p < 0.01$, ***$p < 0.001$ based on two-way ANOVA and the Mann–Whitney U test

TRAP-positive osteoclast formation and NFATc1 expression accompanied by decreasing phos-Y527 SRC and phos-p38 expression. Collectively, these findings suggest that DPP4 expressed in mature osteoclasts plays a crucial role in inflammation-mediated ectopic bone formation in AS pathogenesis, indicating that targeting DPP4 could be a promising therapeutic option.

Bone is a dynamic tissue that constantly changes and regenerates by three consecutive steps: bone resorption by osteoclasts, transition from catabolism to anabolism, and bone formation by osteoblasts. Each step is tightly controlled by molecules mediating communication among bone cells (osteoclasts, osteoblasts, and osteocytes) to maintain bone homeostasis and remodeling. However, an imbalance in bone remodeling leads to various forms of bone disorder such as osteoporosis, osteopenia, osteopetrosis, or AS [44]. Particularly in pathogenesis of AS, there are three serial processes involving in inflammation, bone erosion, and syndesmophyte are observed by radiological changes in ectopic bone formation in enthesis, implicating that regulation of chronic inflammation and resorption by osteoclast to effectively inhibit disease progression in AS [9]. Importantly, osteoclast-derived coupling factors are crucial in bone-related disorders [17] as they release several soluble factors that stimulate osteoblast activity such as platelet-derived growth factor-BB (PDGF-BB), cardiotrophin-1 (CT-1), sphingosine-1-phosphate (S1P), WNT10B, BMP6, and complement factor 3a (C3a) [20, 45–49]. Therefore, controlling osteoclast activity in bone-related disease may have therapeutic potential.

DPP4 inhibitors are commonly used to treat type 2 diabetes. A higher body mass index (BMI) is associated with an increased risk of developing type 2 diabetes. Interestingly, increased BMI is correlated with the presence of syndesmophyte formation and radiographic progression in axial spondyloarthritis, but not in disease activity or inflammation [50, 51]. Moreover, patients with type 2 diabetes have high frequency of osteoporosis and reduced bone mineral density (BMD). Meta-Analysis

exhibited that DPP4 inhibitor use affect positive impact on bone mineral density in patients with type 2 diabetes [52]. Inhibition of soluble DPP4 prevents the release of pro-inflammatory cytokines such as IL-6 and IL-8 [22]. Previous studies reported that DPP4 inhibitors reduce obesity- and macrophage-related inflammation [53, 54]. Conversely, Increased soluble DPP4 exacerbates endothelial inflammation [23]. Furthermore, treatment with DPP4 inhibitor in type 2 diabetes appear to have a low frequency and a decreased disease activity of various autoimmune disease, indicating that DPP4 inhibitors might target pathological immune cells and have therapeutic effects in autoimmune and autoinflammatory diseases [55, 56].

Lipid profiles including total cholesterol, high-density lipoprotein (HDL), low-density lipoprotein (LDL), and triglycerides tends to be decreased levels in AS patients compared to healthy control [57]. The similar results were consistently observed in HLA-B27 transgenic rat [58]. Intriguingly, decreased lipid profiles levels in AS groups were reversed after TNF treatment [59, 60]. DPP4 inhibitors is known to be standard treatment for type 2 diabetic patients via effectively regulating glucose and lipid metabolism and lipid profiles levels, and it could contribute the reduction of cardiovascular risk of these patients [61]. Although we could not be directly assessed in this study, it is reasonable to predict that DPP4 inhibitor groups also might be low levels of lipid profiles and contributes to inflammation-mediated ectopic bone formation of curdlan-injected SKG mice.

We observed that treatment with DPP4 inhibitor reduced murine osteoclastogenesis in bone marrow cells from curdlan-injected SKG mice (Fig. 4E). Previous study reported that a DPP4 inhibitor had potent suppressive effects on the ossification of fibroblasts in AS In contrast, our findings suggest that DPP4 inhibitor treatment did not influence osteoblast differentiation of primary osteoprogenitor cells (Suppl. Figure 6 A ~ 6 H). There was no significant difference of bone-forming activity in osteoblast (Suppl. Figure 6B ~ 6 F) and in the expression of

(See figure on next page.)

Fig. 4 Treatment with DPP4 inhibitor diminishes ectopic bone formation in ankle of curdlan-injected SKG mice in vivo and attenuates osteoclast differentiation in vitro. **A** Representative Micro-CT images of ankles in each group; orange indicates inflamed low-density bones. Red arrows in Micro-CT images indicate ectopic bone formation in the tibia. **B** Low bone density and normal bone density were quantified at the ankle. **C** Histological images of ectopic bone at the tibia stained with H&E (upper), Safranin O (SO; middle), and TRAP (lower). Black arrows in histology images indicate ectopic bone formation in the tibia. **D** The number of TRAP-positive cells was quantified in lower panel of (**C**). Bone marrow of the mice from five weeks after injection of SKG mice with curdlan was isolated to induce murine osteoclast precursor cells (OPCs) with mM-CSF for 2 days and then differentiated into mature osteoclasts in the presence of mM-CSF and mRANKL. OPCs were treated with PBS or DPP4 inhibitor for an additional 4 days. Mature osteoclasts were subjected to (**E**) TRAP staining and (**F**) quantification, (**G**) immunoblotting for DPP4, Phos-Y527 SRC, Phos-Y416 SRC, Total SRC, Phos-p38, Total p38, Phos-ERK, Total ERK, Phos-JNK1/2/3, Total JNK1/2/3 and NFATc1, and β-actin as loading control, and (**H**) RT-qPCR for osteoclast differentiation markers (ITGB3, DC-STAMP, NFATc1, CTK and TRAP; $n = 5$). Representative images are shown. Values are mean ± SEM. Statistical significance is indicated by *$p < 0.05$, **$p < 0.01$, ***$p < 0.001$ after Mann–Whitney U tests

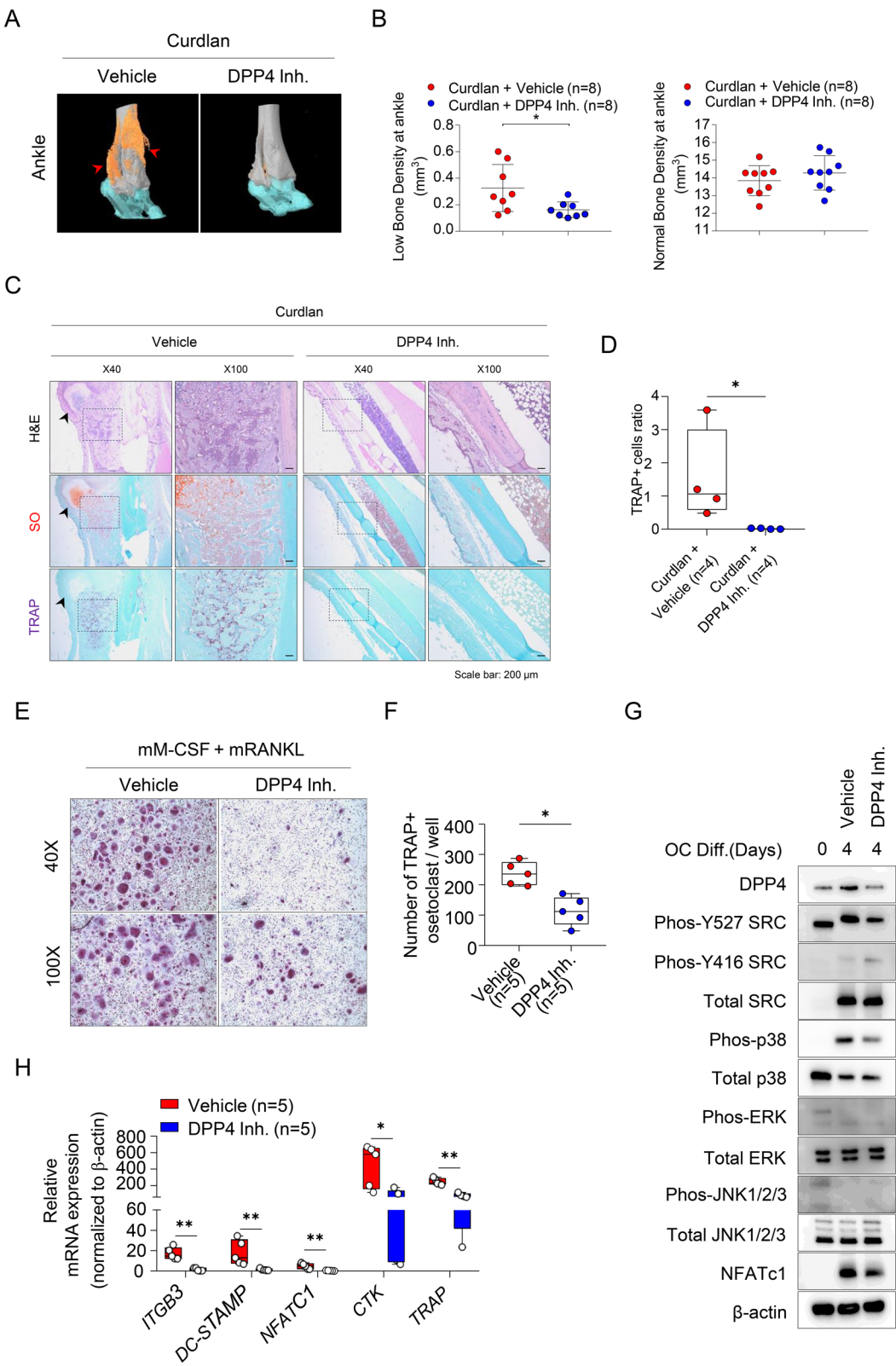**Fig. 4** (See legend on previous page.)

Lee *et al. Arthritis Research & Therapy*   (2025) 27:40

Page 11 of 13

mRNA and protein such as ALP, COL1, OPN, OCN, and RUNX2 (Suppl. Figure 6G and 6 H), indicating that the DPP4 inhibitor selectively regulated osteoclasts differentiation without affecting osteoblasts. Moreover, previous studies have reported that DPP4 is increased in postmenopausal women and correlated with increased bone turnover [20, 62].

Our study has several limitations that should be considered. First, the prevalence of type 2 diabetes among AS patients was not taken into consideration. Although AS treatment reduces inflammation and disease progression, it does not halt bony progression. In our study, we evaluated the effects of a DPP4 inhibitor on arthritis and ectopic bone formation in peripheral joints using a curdlan-injected SKG mice model. Further research is required to investigate the potential preventive effects of DPP4 inhibitors on AS. Second, we did not consider soluble DPP4 levels in vitro and in vivo. DPP4 inhibitors are responsible for inhibiting enzyme activity rather than inhibiting the expression of DPP4. Further research is required to investigate the enzyme activity of DPP4 on AS in vitro and in vivo. Third, we could observe morphological changes in the legs of curdlan-injected SKG mice. However, unfortunately, we did not proceed with leg morphological analysis, as this study focused specifically on the anti-inflammatory effects of inflammation-mediated iso-bone formation and DPP4 inhibitors in SKG mice infused with curdlan at the ankle. It would be necessary to see the change in leg of curdlan-injected SKG mice using footprint analysis in future. Additionally, we did not examine the association between DPP4 and platelet-derived growth factor-BB (PDGF-BB), which is secreted by active osteoclasts and can exacerbate bone mineralization in enthesis cells. Finally, we did not consider disease activity or disease indicators in AS patients when analyzing DPP4 level in serum and synovial fluid samples. Further large-scale multicenter cohort studies are needed to better understand the relationship between type 2 diabetes and AS.

Conclusions

In summary, we demonstrated elevated level of DPP4 in the serum, synovial fluid, and spinal tissues of AS patients. Moreover, DPP4 was highly expressed in osteoclasts, particularly those in the spinal facet joint tissues of AS patients. Inhibition of DPP4 effectively reduced ectopic bone formation and osteoclastogenesis in curdlan-injected SKG mice, both in vivo and in vitro. These findings highlight the potential of DPP4 inhibitors as therapeutic agents for alleviating ectopic bone formation in AS.

Abbreviations

AS	Ankylosing spondylitis
DPP4	Dipeptidyl peptidase-4
PBMCs	Peripheral blood mononuclear cells
OCPs	Osteoclast precursor cells
M-CSF	Macrophage colony-stimulating factor
RANKL	Receptor activator of nuclear factor kappa-B ligand
SKG mice	ZAP-70 mutant SKG mice
Micro-CT	Micro-computed tomography
H&E	Hematoxylin & Eosin
SO	Safranin O
ALP	Alkaline phosphatase
COL	Type 1 collagen
ARS	Alizarin red S
VON	Von kossa
HA	Hydroxyapatite
TRAP	Acid phosphatase 5, tartrate resistant
PDGF-BB	Platelet-derived growth factor-BB
CT-1	Cardiotrophin-1
C3a	Complement factor 3a
S1P	Sphingosine-1-phosphate
BMI	Body mass index
HDL	High-density lipoprotein
LDL	Low-density lipoprotein
BMD	Bone mineral density

Supplementary Information

The online version contains supplementary material available at https://doi.org/10.1186/s13075-025-03474-2.

Supplementary Material 1.

Authors' contributions

All authors contributed to the study conception and design. Material preparation, data collection and analysis were performed by Seung Hoon Lee, Dongju Kim, Chanhyeok Jeon, Min Whangbo, and Hye-Ryeong Jo. Human material resources were collected by Kyu Hoon Lee, Chang-Hun Lee, Sung Hoon Choi, Ye-Soo Park, and Bora Nam. SKG mice were provided by Jeehee Youn. The first draft of the manuscript was written by Kyu Hoon Lee, Sungsin Jo, Tae-Hwan Kim and all authors commented on previous versions of the manuscript. All authors read and approved the final manuscript.

Data availability

No datasets were generated or analysed during the current study.

Declarations

Ethics approval and consent to participate

For human materials, this study was approved by the ethics committee of Hanyang University Seoul Hospital, and written informed consent was obtained from all study participants (2014-05-002 and 2023-06-048). For animal, all experimental procedures were performed in accordance with the Guide for the Care and Use of Laboratory Animals and were approved by the Animals Ethics Screening Committee of Hanyang University (2022–0027A).

Consent for publication

Not applicable.

Competing interests

The authors declare no competing interests.

Lee *et al. Arthritis Research & Therapy*   (2025) 27:40

Page 12 of 13

Author details
[1]Hanyang University Institute for Rheumatology Research (HYIRR), Hanyang University, Seoul 04763, Korea. [2]Department of Rehabilitation Medicine, Hanyang University Hospital for Rheumatic Diseases, Seoul 04763, Korea. [3]Department of Anatomy & Cell Biology, College of Medicine, Hanyang University, Seoul 04763, South Korea. [4]Department of Orthopaedic Surgery, Hanyang University Seoul Hospital, Seoul 04763, South Korea. [5]Department of Orthopaedic Surgery, Guri Hospital, Hanyang University College of Medicine, Guri 11923, South Korea. [6]Department of Rheumatology, Hanyang University Hospital for Rheumatic Diseases, 222-1 Wangsimni-ro, Seongdong-gu, Seoul 04763, Republic of Korea. [7]Department of Biology, College of Natural Sciences, Soonchunhyang University, 22 Soonchunhyang-ro, Shinchang-myeon, Asan city, Chungcheongnam-do 31538, Republic of Korea.

References
1. Zhu W, He X, Cheng K, Zhang L, Chen D, Wang X, Qiu G, Cao X, Weng X. Ankylosing spondylitis: etiology, pathogenesis, and treatments. Bone Res. 2019;7:22.
2. Inman RD. Axial spondyloarthritis: current advances, future challenges. J Rheum Dis. 2021;28(2):55–9.
3. Ward MM, Deodhar A, Gensler LS, Dubreuil M, Yu D, Khan MA, Haroon N, Borenstein D, Wang R, Biehl A, et al. 2019 update of the American College of Rheumatology/Spondylitis Association of America/Spondyloarthritis Research and Treatment Network Recommendations for the treatment of Ankylosing spondylitis and Nonradiographic Axial Spondyloarthritis. Arthritis Rheumatol. 2019;71(10):1599–613.
4. Haroon N, Inman RD, Learch TJ, Weisman MH, Lee M, Rahbar MH, Ward MM, Reveille JD, Gensler LS. The impact of tumor necrosis factor alpha inhibitors on radiographic progression in ankylosing spondylitis. Arthritis Rheum. 2013;65(10):2645–54.
5. Koo BS, Oh JS, Park SY, Shin JH, Ahn GY, Lee S, Joo KB, Kim TH. Tumour necrosis factor inhibitors slow radiographic progression in patients with ankylosing spondylitis: 18-year real-world evidence. Ann Rheum Dis. 2020;79(10):1327–32.
6. Abate MV, Sandrin C, Pastore S. Secukinumab for ankylosing spondylitis. Lancet. 2014;383(9919):780.
7. Baeten D, Baraliakos X, Braun J, Sieper J, Emery P, van der Heijde D, McInnes I, van Laar JM, Landewe R, Wordsworth P, et al. Anti-interleukin-17A monoclonal antibody secukinumab in treatment of ankylosing spondylitis: a randomised, double-blind, placebo-controlled trial. Lancet. 2013;382(9906):1705–13.
8. Baraliakos X, Listing J, Rudwaleit M, Sieper J, Braun J. The relationship between inflammation and new bone formation in patients with ankylosing spondylitis. Arthritis Res Ther. 2008;10(5):R104.
9. Tam LS, Gu J, Yu D. Pathogenesis of ankylosing spondylitis. Nat Rev Rheumatol. 2010;6(7):399–405.
10. Schett G, Stolina M, Dwyer D, Zack D, Uderhardt S, Kronke G, Kostenuik P, Feige U. Tumor necrosis factor alpha and RANKL blockade cannot halt bony spur formation in experimental inflammatory arthritis. Arthritis Rheum. 2009;60(9):2644–54.
11. Tseng HW, Pitt ME, Glant TT, McRae AF, Kenna TJ, Brown MA, Pettit AR, Thomas GP. Inflammation-driven bone formation in a mouse model of ankylosing spondylitis: sequential not parallel processes. Arthritis Res Ther. 2016;18:35.
12. Yu T, Zhang J, Zhu W, Wang X, Bai Y, Feng B, Zhuang Q, Han C, Wang S, Hu Q, et al. Chondrogenesis mediates progression of ankylosing spondylitis through heterotopic ossification. Bone Res. 2021;9(1):19.
13. Jo S, Lee SH, Park J, Nam B, Kim H, Youn J, Lee S, Kim TJ, Sung IH, Choi SH, et al. Platelet-derived growth factor B is a key element in the pathological bone formation of Ankylosing Spondylitis. J Bone Min Res. 2023;38(2):300–12.
14. Boyle WJ, Simonet WS, Lacey DL. Osteoclast differentiation and activation. Nature. 2003;423(6937):337–42.
15. Ikebuchi Y, Aoki S, Honma M, Hayashi M, Sugamori Y, Khan M, Kariya Y, Kato G, Tabata Y, Penninger JM, et al. Coupling of bone resorption and formation by RANKL reverse signalling. Nature. 2018;561(7722):195–200.
16. Kong YY, Yoshida H, Sarosi I, Tan HL, Timms E, Capparelli C, Morony S, Oliveira-dos-Santos AJ, Van G, Itie A, et al. OPGL is a key regulator of osteoclastogenesis, lymphocyte development and lymph-node organogenesis. Nature. 1999;397(6717):315–23.
17. Henriksen K, Karsdal MA, Martin TJ. Osteoclast-derived coupling factors in bone remodeling. Calcif Tissue Int. 2014;94(1):88–97.
18. Kim BJ, Lee YS, Lee SY, Baek WY, Choi YJ, Moon SA, Lee SH, Kim JE, Chang EJ, Kim EY, et al. Osteoclast-secreted SLIT3 coordinates bone resorption and formation. J Clin Invest. 2018;128(4):1429–41.
19. Su W, Liu G, Liu X, Zhou Y, Sun Q, Zhen G, Wang X, Hu Y, Gao P, Demehri S, et al. Angiogenesis stimulated by elevated PDGF-BB in subchondral bone contributes to osteoarthritis development. JCI Insight. 2020;5(8):e135446.
20. Xie H, Cui Z, Wang L, Xia Z, Hu Y, Xian L, Li C, Xie L, Crane J, Wan M, et al. PDGF-BB secreted by preosteoclasts induces angiogenesis during coupling with osteogenesis. Nat Med. 2014;20(11):1270–8.
21. Drucker DJ. Glucagon-like peptides. Diabetes. 1998;47(2):159–69.
22. Wronkowitz N, Gorgens SW, Romacho T, Villalobos LA, Sanchez-Ferrer CF, Peiro C, Sell H, Eckel J. Soluble DPP4 induces inflammation and proliferation of human smooth muscle cells via protease-activated receptor 2. Biochim Biophys Acta. 2014;1842(9):1613–21.
23. Liu C, Xu J, Fan J, Liu C, Xie W, Kong H. DPP-4 exacerbates LPS-induced endothelial cells inflammation via integrin-alpha5beta1/FAK/AKT signaling. Exp Cell Res. 2024;435(1):113909.
24. Conarello SL, Li Z, Ronan J, Roy RS, Zhu L, Jiang G, Liu F, Woods J, Zycband E, Moller DE, et al. Mice lacking dipeptidyl peptidase IV are protected against obesity and insulin resistance. Proc Natl Acad Sci U S A. 2003;100(11):6825–30.
25. Napoli N, Chandran M, Pierroz DD, Abrahamsen B, Schwartz AV, Ferrari SL, Bone IOF, Diabetes Working G. Mechanisms of diabetes mellitus-induced bone fragility. Nat Rev Endocrinol. 2017;13(4):208–19.
26. Ustulin M, Park SY, Choi H, Chon S, Woo JT, Rhee SY. Effect of dipeptidyl Peptidase-4 inhibitors on the risk of bone fractures in a Korean population. J Korean Med Sci. 2019;34(35): e224.
27. Schwartz AV, Vittinghoff E, Bauer DC, Hillier TA, Strotmeyer ES, Ensrud KE, Donaldson MG, Cauley JA, Harris TB, Koster A, et al. Association of BMD and FRAX score with risk of fracture in older adults with type 2 diabetes. JAMA. 2011;305(21):2184–92.
28. Monami M, Dicembrini I, Antenore A, Mannucci E. Dipeptidyl peptidase-4 inhibitors and bone fractures: a meta-analysis of randomized clinical trials. Diabetes Care. 2011;34(11):2474–6.
29. Nishida H, Suzuki H, Madokoro H, Hayashi M, Morimoto C, Sakamoto M, Yamada T. Blockade of CD26 signaling inhibits human osteoclast development. J Bone Min Res. 2014;29(11):2439–55.
30. Weivoda MM, Chew CK, Monroe DG, Farr JN, Atkinson EJ, Geske JR, Eckhardt B, Thicke B, Ruan M, Tweed AJ, et al. Identification of osteoclast-osteoblast coupling factors in humans reveals links between bone and energy metabolism. Nat Commun. 2020;11(1):87.
31. Ishida M, Shen WR, Kimura K, Kishikawa A, Shima K, Ogawa S, Qi J, Ohori F, Noguchi T, Marahleh A, et al. DPP-4 inhibitor impedes lipopolysaccharide-induced osteoclast formation and bone resorption in vivo. Biomed Pharmacother. 2019;109:242–53.
32. Yang Y, Zhao C, Liang J, Yu M, Qu X. Effect of dipeptidyl Peptidase-4 inhibitors on bone metabolism and the possible underlying mechanisms. Front Pharmacol. 2017;8: 487.
33. van der Linden S, Valkenburg HA, Cats A. Evaluation of diagnostic criteria for ankylosing spondylitis. A proposal for modification of the New York criteria. Arthritis Rheum. 1984;27(4):361–8.
34. Altman R, Asch E, Bloch D, Bole G, Borenstein D, Brandt K, Christy W, Cooke TD, Greenwald R, Hochberg M, et al. Development of criteria for the classification and reporting of osteoarthritis. Classification of osteoarthritis of the knee. Diagnostic and Therapeutic Criteria Committee of the American Rheumatism Association. Arthritis Rheum. 1986;29(8):1039–49.
35. Jo S, Wang SE, Lee YL, Kang S, Lee B, Han J, Sung IH, Park YS, Bae SC, Kim TH. IL-17A induces osteoblast differentiation by activating JAK2/STAT3 in ankylosing spondylitis. Arthritis Res Ther. 2018;20(1):115.
36. Jo S, Nam B, Lee YL, Park H, Weon S, Choi SH, Park YS, Kim TH. The TNF-NF-kB-DKK1 Axis promoted bone formation in the enthesis of Ankylosing Spondylitis. J Rheum Dis. 2021;28(4):216–24.
37. Oh Y, Park R, Kim SY, Park SH, Jo S, Kim TH, Ji JD. B7-H3 regulates osteoclast differentiation via type I interferon-dependent IDO induction. Cell Death Dis. 2021;12(11):971.

38. Jeon C, Jang Y, Lee SH, Weon S, Park H, Lee S, Oh Y, Choi SH, Wang SE, Kim TH, et al. Abnormal kynurenine level contributes to the pathological bone features of ankylosing spondylitis. Int Immunopharmacol. 2023;118:110132.

39. Jo S, Lee SH, Jeon C, Jo HR, Ko E, Whangbo M, Kim TJ, Park YS, Kim TH. Elevated BMPR2 expression amplifies osteoblast differentiation in ankylosing spondylitis. J Rheum Dis. 2023;30(4):243–50.

40. Sakaguchi N, Takahashi T, Hata H, Nomura T, Tagami T, Yamazaki S, Sakihama T, Matsutani T, Negishi I, Nakatsuru S, et al. Altered thymic T-cell selection due to a mutation of the ZAP-70 gene causes autoimmune arthritis in mice. Nature. 2003;426(6965):454–60.

41. Ruutu M, Thomas G, Steck R, Degli-Esposti MA, Zinkernagel MS, Alexander K, Velasco J, Strutton G, Tran A, Benham H, et al. Beta-glucan triggers spondylarthritis and Crohn's disease-like ileitis in SKG mice. Arthritis Rheum. 2012;64(7):2211–22.

42. Lee JH, Lee SH, Jeon C, Han J, Kim SH, Youn J, Park YS, Kim TJ, Kim JS, Jo S, et al. The complement factor H-related protein-5 (CFHR5) exacerbates pathological bone formation in ankylosing spondylitis. J Mol Med (Berl). 2024;102(4):571–83.

43. Benham H, Rehaume LM, Hasnain SZ, Velasco J, Baillet AC, Ruutu M, Kikly K, Wang R, Tseng HW, Thomas GP, et al. Interleukin-23 mediates the intestinal response to microbial beta-1,3-glucan and the development of spondyloarthritis pathology in SKG mice. Arthritis Rheumatol. 2014;66(7):1755–67.

44. Feng X, McDonald JM. Disorders of bone remodeling. Annu Rev Pathol. 2011;6:121–45.

45. Sims NA, Martin TJ. Coupling signals between the Osteoclast and osteoblast: how are messages transmitted between these temporary visitors to the bone surface? Front Endocrinol (Lausanne). 2015;6:41.

46. Walker EC, McGregor NE, Poulton IJ, Pompolo S, Allan EH, Quinn JM, Gillespie MT, Martin TJ, Sims NA. Cardiotrophin-1 is an osteoclast-derived stimulus of bone formation required for normal bone remodeling. J Bone Min Res. 2008;23(12):2025–32.

47. Ryu J, Kim HJ, Chang EJ, Huang H, Banno Y, Kim HH. Sphingosine 1-phosphate as a regulator of osteoclast differentiation and osteoclast-osteoblast coupling. EMBO J. 2006;25(24):5840–51.

48. Pederson L, Ruan M, Westendorf JJ, Khosla S, Oursler MJ. Regulation of bone formation by osteoclasts involves Wnt/BMP signaling and the chemokine sphingosine-1-phosphate. Proc Natl Acad Sci U S A. 2008;105(52):20764–9.

49. Matsuoka K, Park KA, Ito M, Ikeda K, Takeshita S. Osteoclast-derived complement component 3a stimulates osteoblast differentiation. J Bone Min Res. 2014;29(7):1522–30.

50. Kim SK, Choe JY, Lee SS, Shin K. Body mass index is related with the presence of syndesmophyte in axial spondyloarthritis: data from the Korean College of Rheumatology BIOlogics (KOBIO) registry. Mod Rheumatol. 2017;27(5):855–61.

51. Roberts MJ, Leonard AN, Bishop NC, Moorthy A. Lifestyle modification and inflammation in people with axial spondyloarthropathy-A scoping review. Musculoskelet Care. 2022;20(3):516–28.

52. Huang L, Zhong W, Liang X, Wang H, Fu SE, Luo Z. Meta-analysis on the association between DPP-4 inhibitors and bone mineral density and osteoporosis. J Clin Densitom. 2024;27(1):101455.

53. Ta NN, Li Y, Schuyler CA, Lopes-Virella MF, Huang Y. DPP-4 (CD26) inhibitor alogliptin inhibits TLR4-mediated ERK activation and ERK-dependent MMP-1 expression by U937 histiocytes. Atherosclerosis. 2010;213(2):429–35.

54. Dobrian AD, Ma Q, Lindsay JW, Leone KA, Ma K, Coben J, Galkina EV, Nadler JL. Dipeptidyl peptidase IV inhibitor sitagliptin reduces local inflammation in adipose tissue and in pancreatic islets of obese mice. Am J Physiol Endocrinol Metab. 2011;300(2):E410-421.

55. Kim SC, Schneeweiss S, Glynn RJ, Doherty M, Goldfine AB, Solomon DH. Dipeptidyl peptidase-4 inhibitors in type 2 diabetes may reduce the risk of autoimmune diseases: a population-based cohort study. Ann Rheum Dis. 2015;74(11):1968–75.

56. Huang J, Liu X, Wei Y, Li X, Gao S, Dong L, Rao X, Zhong J. Emerging role of dipeptidyl Peptidase-4 in autoimmune disease. Front Immunol. 2022;13:830863.

57. Mathieu S, Gossec L, Dougados M, Soubrier M. Cardiovascular profile in ankylosing spondylitis: a systematic review and meta-analysis. Arthritis Care Res (Hoboken). 2011;63(4):557–63.

58. Furesi G, Fert I, Beaufrere M, Araujo LM, Glatigny S, Baschant U, von Bonin M, Hofbauer LC, Horwood NJ, Breban M, et al. Rodent models of spondyloarthritis have decreased white and bone marrow adipose tissue depots. Front Immunol. 2021;12: 665208.

59. van Eijk IC, de Vries MK, Levels JH, Peters MJ, Huizer EE, Dijkmans BA, van der Horst-Bruinsma IE, Hazenberg BP, van de Stadt RJ, Wolbink GJ, et al. Improvement of lipid profile is accompanied by atheroprotective alterations in high-density lipoprotein composition upon tumor necrosis factor blockade: a prospective cohort study in ankylosing spondylitis. Arthritis Rheum. 2009;60(5):1324–30.

60. van Halm VP, van Denderen JC, Peters MJ, Twisk JW, van der Paardt M, van der Horst-Bruinsma IE, van de Stadt RJ, de Koning MH, Dijkmans BA, Nurmohamed MT. Increased disease activity is associated with a deteriorated lipid profile in patients with ankylosing spondylitis. Ann Rheum Dis. 2006;65(11):1473–7.

61. Monami M, Lamanna C, Desideri CM, Mannucci E. DPP-4 inhibitors and lipids: systematic review and meta-analysis. Adv Ther. 2012;29(1):14–25.

62. Kim H, Baek KH, Lee SY, Ahn SH, Lee SH, Koh JM, Rhee Y, Kim CH, Kim DY, Kang MI, et al. Association of circulating dipeptidyl-peptidase 4 levels with osteoporotic fracture in postmenopausal women. Osteoporos Int. 2017;28(3):1099–108.

Publisher's Note